



## DEVELOPING FRAGILITY CURVES FOR TYPICAL RESIDENTIAL BUILDING STOCK IN THE STATE OF ISRAEL

Y. Daniel <sup>(1)</sup>, A. Kagermanov <sup>(2)</sup>, Y. Offir <sup>(3)</sup>,

<sup>(1)</sup> Earthquake Engineering Specialist, Yaron Offir Engineers, [yael.daniel@yoe.co.il](mailto:yael.daniel@yoe.co.il)

<sup>(2)</sup> Researcher, Institute for Advanced Studies, Pavia (IUSS), [alexander.kagermanov@iusspavia.it](mailto:alexander.kagermanov@iusspavia.it)

<sup>(3)</sup> Partner, Yaron Offir Engineers, [aron@yoe.co.il](mailto:aron@yoe.co.il)

### Abstract

As part of its effort to prepare for an upcoming seismic event, the National Israeli Seismic Preparedness Steering Committee (NISPSC) decided to update the HAZUS models used for seismic vulnerability assessment and loss estimation on a national level, from using US-based building type fragility curves to using locally- based building type fragility curves, thus allowing a more accurate and relevant loss estimation process. This, in turn, enables improved decision making on a State or local level, and better seismic preparedness on the Governmental level.

This paper presents the results of a two year research project funded by the NISPSC to develop fragility curves for typical building types which represent a large section of the building stock in the State of Israel. As part of the first stage of the project, and based on a study carried out to identify the existing building stock and its characteristics, 4 typical building types, representative of a large total percentage of the local building stock, were selected. These included mid-rise RC building types A, B, C and a precast building type D, designed for gravity loads only, and featuring different structural deficiencies such as weak/ soft stories, short columns, brittle connections, lack of ductile detailing, in-plan torsion, etc.

Fragility curve development included nonlinear finite element modeling of the abovementioned building types, which attempted to realistically feature critical structural deficiencies of each building typology. Derivation of fragility curves was based on nonlinear static analysis (pushover) and the capacity spectrum method according to the HAZUS methodology. The assessment was performed under increasing levels of ground motion intensity, inducing different damage states ranging from light damage to complete collapse. A statistical treatment of the results was undertaken in order to incorporate the variability in the capacity and demand, and subsequently calculate the fragility curves, i.e. the probabilities of reaching or exceeding a certain damage state given the seismic hazard. The fragility curves derived were compared to similar US-based fragility curves, where available. Comparison showed the difference in behavior between the Israeli building typology and the US counterpart, further assuring the need to replace US-based fragilities used in the current Israeli loss estimation process, to local fragilities, representing local building stock.

**Keywords:** seismic analysis, fragility assessment, HAZUS, building stock.



## 1. Introduction

The State of Israel is located in an area which is known to be a relatively seismically active area, and is situated between the African, Asian and Euro-Asian tectonic plates. The eastern border of the State of Israel aligns with the African-Arabian fault line, which is the most active (but not only) fault line affecting the seismicity of the region. The two sides of the African-Arabian fault line (known as the Dead Sea Transform) transform one against the other, both moving north, with the eastern side moving at a faster pace than the western side, resulting in a relative velocity of about 4 mm/year. Historic information, based on a verity of sources, shows that, statistically speaking, a relatively strong ground motion is expected every 80-100 years. The last strong earthquake to occur within country borders dates back to 1927, thus a potentially strong event is due at any given time. Israel's building stock is partially aging, as many buildings were built together with the country's population boosts in the 1950's and 1960's. These ageing structures suffer from deterioration, which, together with growing population rates (over 9,000,000 people in 2019), raises the concern for a possibly significant hazard.

As part of national seismic preparedness plans, estimates on the expected damage and loss are published. The Israeli National Seismic Preparedness Steering Committee (NSPSC)'s current preparedness framework for national agencies, ministries, and authorities to prepare for, state the following loss and damage levels: 7,000 casualties, 8,600 people severely injured, 37,000 people lightly injured, 170,000 homeless/ with no shelter, 9,500 people trapped in structures, 28,600 buildings heavily or completely damaged (over 45% damage to building value), 290,000 buildings lightly to moderately damaged. The state of Israel has a large building stock built over several decades, both before and after the introduction of a seismic code in the late 1970s/ early 1980s. On the State level, current damage and loss estimation practice and predictions are based on models and information compatible to United States (US) building stock, as opposed to, to local building characteristics. Therefore, it can be said that there is considerable deviation between current damage and loss estimation and damage that is likely to occur following a seismic event in the region. To improve estimation and obtain a more realistic pictures as to the expected damage (injuries, casualties, losses) there is a need to update models in a way that considers local building stock characteristics, with regards to relevant building typologies, materials, construction methods, etc. These can be relatively easily accounted for via development of new fragility curves, based on the behavior of local building typologies recognized.

This paper presents the derivation of fragility curves and parameters for three building typologies, which represent common Israeli building types. Building topologies were selected as part of the first stage of a local HAZUS update project, and are based on a study carried out to identify the characteristics of existing local building stock. These typical building types included mid-rise reinforced concrete (RC) buildings and a precast building designed for gravity loads only. The different buildings represent common structural deficiencies, with respect to seismic behavior, such as weak/ soft stories, short columns, brittle connections, lack of ductile detailing, in-plan torsion, etc. Where possible, the fragility curves developed were compared to their HAZUS counterparts, and differences found reveal the lack of conservativeness when using US-based parameters, thus highlighting the need in updating parameters used for local vulnerability assessment and damage and loss estimation models, so as to allow a more realistic national preparedness frame, which is long overdue.

## 2. Project definition and objectives

HAZUS [1] is a software which is used for damage and loss estimation based on natural hazards such as earthquakes, widely used in practice in the US and worldwide. HAZUS contains a package of predefined fragility curves which were derived over decades of research and analytical studies, and are compatible mostly to typical US construction.

Studies have shown that using HAZUS curves for buildings outside of the USA is questionable as per its ability to realistically represent structural behavior during and after a ground motion [2, 3, 4]. Israel's building stock, as opposed to its US counterpart is mainly comprised of RC structures. The HAZUS platform currently has 9 options for RC structures: C1L, C1M, C1H (for concrete frame structures with no infill), C2L,



C2M, C2H (for concrete structures with shear walls), and C3L, C3M, C3H (for concrete frame structures with infill walls). Structures are categorized based on height/ number of floors (1-2, 4-7, 8+). These options are quite limited, and are questionable as per their ability to characterize Israeli building stock. For vulnerability assessment, the HAZUS building stock is classified to one of 4 groups, which represent their potential resistance to seismic loads: High Code, Moderate Code, Low Code, and Pre Code. Classification into groups is based on assumptions on the expected seismic resistance of the structure, which is based on a combination between: (a) its age- relevant to seismic codes available at time of construction, and (b) seismicity of the region where built. Again, it is questionable whether these categories are relevant to local building stock.

The objective of the project defined and initiated by the Israeli NSPSC, is, therefore, to replace/ update fragility curves given in the HAZUS software module to curves compatible to Israeli building practice. Project goals included:

- a. Identification of a small amount of structure types/ typologies (with reference to similar geometry, lateral system, height, etc), with realization that this phase of the project will not fully represent local building stock, and thus will not allow the most accurate damage estimation possible, but rather it will allow a considerable improvement in damage estimations with respect to current practice, at a relatively small investment of funds and time.
- b. For these typologies, production of new fragility curves, which are based on nonlinear analyses under increasing levels of seismic hazard intensities, in combination with capacity- spectrum method to compute performance points for different damage states of interest.
- c. The intention is to use fragility parameters computed to replace parameters currently used in HAZUS' damage and loss estimation module. This will allow using the same national damage and loss estimation methodology and procedure currently used, while improving its accuracy by using parameters that better represent local building inventory.
- d. Pilot project included definition and study of 4 specific building types.

### 3. Fragility assessment and curve derivation

The objective is to create fragility curves for different typologies of residential buildings typically found in the State of Israel, following the HAZUS methodology. The HAZUS methodology is used for the derivation of such fragility curves, and is based on nonlinear static analysis (pushover) and the capacity spectrum method (CSM) [5] for the assessment seismic performance. This assessment is performed under increasing levels of ground motion intensity, which will cause different damage states (DS) ranging from light damage to complete collapse. A statistical treatment of the results is required in order to incorporate the variability in the capacity and the demand. The final results are fragility curves, which indicate the probability of reaching or exceeding a certain DS given the seismic hazard.

#### 3.1. Definition of damage states

Four DSs were adopted from HAZUS: Slight Structural Damage (“S”), Moderate Structural Damage (“M”), Extensive Structural Damage (“E”), and Complete Structural Damage (“C”). The exact description for each DS can be found in HAZUS manuals, and is dependent on building type.

#### 3.2. Capacity curve derivation

Eigenvalue analysis is performed in order to determine the fundamental period and mode shapes of the structure. This information is used to calculate the modal participation factor and base shear factor, which are used as part of the capacity spectrum method. Lateral load vectors for pushover analysis are defined as the mass matrix multiplied by a vector proportional to the first mode shape of the structure.

Pushover analysis in each of two main directions is performed, as the vector of lateral forces is distributed along the height at each floor center of mass. The top displacement is chosen as the controlling degree of freedom. Collapse mechanisms are determined based on building behavior. Shear and bending



capacities are determined for the different elements, so as to estimate demand-capacity ratios for the various elements. The maximum inter-story drift ratio (IDR) damage thresholds associated with each DS are identified on the global pushover curves.

Uncertainty in the capacity is caused by the variability in material properties. Compressive strength of concrete ( $f_c$ ) and yield strength of steel ( $f_y$ ) are assumed to be randomly distributed. This information is used to generate a sample of structures with random distributions of  $f_c$  and  $f_y$ . The Latin Hypercube Sampling technique is used for this purpose. In this technique, the random variable domain is subdivided into a finite number of non-overlapping intervals, such that each interval has the same probability (i.e. same area under the probability density function). Next, a random number from 0 to 1 is assigned to each interval. This number is used to calculate the probability of exceedance for each interval. For this study, 10 non-overlapping intervals were used, with a probability of 0.1 for each interval. This results in a sample of 10 structures with randomly distributed  $f_c$  and  $f_y$  properties. As a final step, the values of  $f_c$  and  $f_y$  are randomly paired. Pushover analyses are performed for each individual sample structure.

The CSM [5] is used for performance evaluation under different earthquake damage scenarios. The objective is to find the performance point for each one of the structures previously defined, in each direction and for each set of scaled ground motions. The performance point thus obtained can be associated to its corresponding DS through the maximum IDR. First, the CSM requires transformation of the MDOF pushover curve to the SDOF curve in the spectral acceleration – spectral displacement domain. Next, bi-linearization of the capacity curve is required. This is performed for each pushover curve based on the equal energy approach. The ultimate displacement is defined at the peak base shear, or at 90% post-peak strength reduction of the pushover curve. Finally, the performance point is found at the intersection between the ground motion response spectrum and the bilinear pushover curve. This process is performed iteratively until the damping coefficient is the same in both systems. The damping coefficient of the structural system is adjusted to account for hysteretic damping. Once the performance point is found, the corresponding maximum IDR can be obtained, and the DS can be classified according to levels defined in HAZUS.

### 3.3. Derivation of HAZUS-compatible fragility curves

The medians ( $S_{d,DS}$ ) and lognormal standard deviation ( $\beta$ ) for each damage level can be obtained from the moment estimates of the spectral displacements at the performance point. These are computed using Eqs. (1)-(2):

$$\ln S_{d,DS} = \sum \ln S_{di} / N \quad (1)$$

$$\beta_{C,D} = \sqrt{\sum (\ln S_{di} - \ln S_{d,DS})^2 / (N-1)} \quad (2)$$

where  $N$  is the total number of counts for the corresponding DSs. The standard deviation  $\beta_{C,D}$  accounts for the variability in the demand and capacity. According to HAZUS, the total lognormal standard deviation computed using Eq. (3):

$$\beta_{DS} = \sqrt{\text{CONV}(\beta_C, \beta_D)^2 + \beta_{T,DS}^2} \quad (3)$$

where  $\beta_{T,DS}$  corresponds to the variability in the threshold of the DS (assumed herein as 0.4). The term  $\text{CONV}(\beta_C, \beta_D)$  considers the combined variability in the demand and capacity, and it corresponds to  $\beta_{C,D}$  obtained from analysis. Finally, the probability of exceeding a certain DS, used to build the fragility curve can be expressed in terms of the standard normal distribution function,  $\Phi$ , as shown in Eq. (4):

$$P(X \leq S_d | DS) = \Phi \left[ \frac{1}{\beta_{DS}} \ln \left( \frac{S_d}{S_{d,DS}} \right) \right] \quad (4)$$



## 4. Results- fragility derivation

### 4.1. Building typology A

The building is a 4-storey RC frame with infills and waffle slabs, shown in Fig. 1. No infills are present at the ground level, creating a soft-story configuration prone to failure. Column cross-sections are 20x40 cm<sup>2</sup> at the ground level and 20x25 cm<sup>2</sup> above ground, with center-to-center spans varying between 2.7-4.3m. Perimeter beams are present in both directions, with cross-sections ranging between 27x36 cm<sup>2</sup> and 13x45 cm<sup>2</sup>. Waffle slabs consist of 12-14cm ribs with 5cm topping, spanning in the north-to-south direction, 3cm of sand and 2cm of paving, and 10-12cm wide ribs depending on the floor level. Infill panels consist of unreinforced hollow-core concrete blocks. In the front frame (Fig. 2), infill panels present vertical openings, which does not allow the formation of a diagonal compression strut since this requires the lateral support of the column. In the lateral perimeter frames, full infill panels are present, which will be taken into account in the numerical model. Although several walls seem to be present, including a U-shaped wall around the staircase, these are treated as part of the gravity loading systems. For structural walls to be part of the lateral load resisting system strict requirements have to be met in terms of wall-to-foundation connection and wall-to-slab connection, in addition to ductile detailing of the boundary and web regions of the wall. This is not usually the case for gravity-load designed frames. The infill panels are assumed consisting of unconfined concrete masonry blocks of dimensions 100x100x200 mm with cement mortar applied in the bed and head joints.

The material properties for steel and concrete were obtained from site investigation. The concrete compressive strength and yield strength of steel are assumed to be randomly distributed, with means and standard deviations of  $\mu_{f_c}=30\text{MPa}$ ,  $\sigma_{f_c}=5.25\text{MPa}$  for  $f_c$ , and  $\mu_{f_y}=226\text{MPa}$ ,  $\sigma_{f_y}=24\text{MPa}$  for  $f_y$ . 10 different sets of strengths were used for analysis.

Seismic hazard was obtained from probabilistic site-specific assessment. Seven natural records were selected for the present study. The selection criteria was based on minimizing the logarithmic difference between the candidate and target acceleration spectra in an average sense. The selected ground motions will be used in the derivation of fragility curves.

According to HAZUS, the present building can be classified as mid-rise “Concrete frame with unreinforced masonry walls” (group category C3M). This is a “composite” structural system where the initial lateral resistance is provided by the infill walls. Upon cracking of the infills, further lateral resistance is provided by the concrete frame “braced” by the infill acting as diagonal compression struts. Collapse of the structure results when the infill walls disintegrate (due to compression failure of the masonry “struts”) and the frame loses stability, or when the concrete columns suffer shear failures due to reduced effective height and the high shear forces imposed on them by the masonry compression struts.

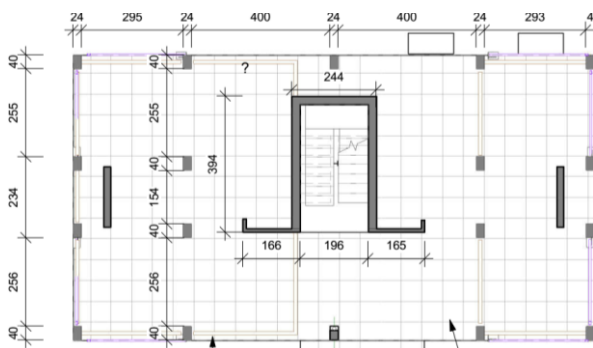


Fig. 1- Building plan configuration, typology A

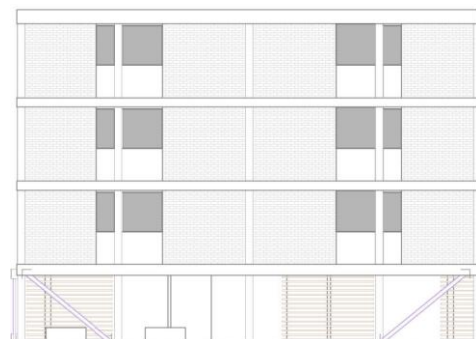


Fig. 2 Building elevation, , typology A



The structure was modeled using the finite-element (FE) software IDEEA [6], which accounts for geometric and material nonlinearities. Columns are modeled with nonlinear frame elements, with the cross-section discretized into 100 fibers at which the constitutive laws for steel and concrete are applied. Similarly, beams were modeled with nonlinear frame elements and fiber-cross section discretization to account for possible plastic hinging. For the floors rigid diaphragm action was assumed. Infills were explicitly taken into account in the analysis. These were modeled with equivalent diagonal struts which can carry compression forces only.

Results from pushover analysis are shown in Fig. 3, where the top displacement was chosen as the controlling degree of freedom. From **Error! Reference source not found.** it can be noticed that the response in the X direction is more flexible, with a lower capacity but higher ductility. In the Y direction the response is stiffer, with a higher capacity but a much lower ductility. This difference in response is mainly due to the orientation of the columns (strong axis in the Y direction), which provides more lever arm to the tension reinforcement, and therefore higher bending moment capacity. Also, the presence of infills affects the response. The collapse mechanisms are shown in Fig. 4. In both directions a soft-story develops above the ground level, with plastic hinging at top and bottom of the columns.

The maximum IDR damage thresholds associated with each DS were identified on the global pushover curves following the criteria in section 3.1, and were defined as: (a) slight damage at first cracking, (b) moderate damage at global yield point, (c) extensive damage at maximum base shear, and (d) complete damage at 10% post-peak strength reduction. The above damage thresholds were associated to a maximum IDR, which was used as the engineering demand parameter (EDP) in the derivation of fragility curves. In Fig. 5, the five DSs are highlighted, where “ND” indicates no damage, “S”- slight damage, “M”- moderate damage, “E”- extensive damage, and “C”- complete damage. The maximum IDR thresholds associated with each DS are summarized below. In the Y-direction, a redefinition of “M” and “E” DSs was required, since the pushover curve does not present a clear post-peak response. The “M” DS was assumed between the global yield point and 0.75% IDR, whereas the “E” DS was assumed between 0.75% and the peak response. This resulted in: 0.2%- “S”, 0.5%- “M”, 1.0%- “E”, 2.5%- “C”- in the X direction, and 0.1%- “S”, 0.2%- “M”, 0.8%- “E”, 2.0%- “C”- in the Y direction.

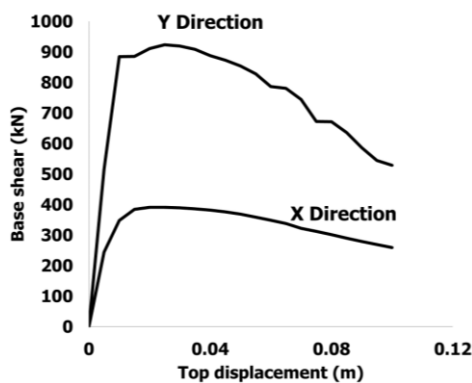


Fig. 3- Pushover curve, typology A

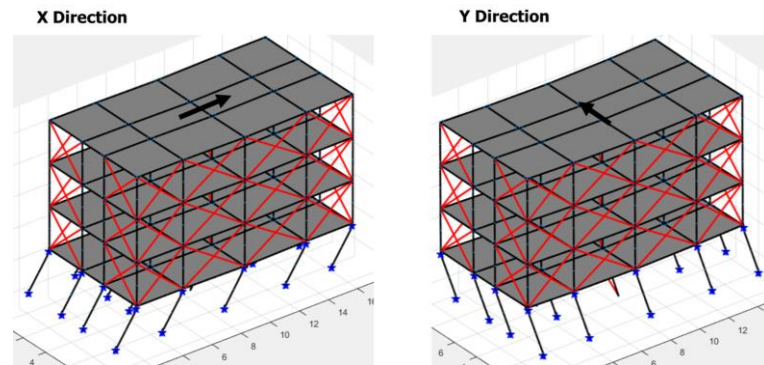


Fig. 4- Soft-story mechanisms at global failure

CSM was used for performance evaluation under different earthquake damage scenarios, where the performance point for each one of the ten sample structures previously defined, in each direction and for each set of seven scaled ground motions, was computed, and associated to its corresponding DS through the maximum IDR, as explained in section 3.2.

The medians and lognormal standard deviation for each damage level were obtained from the moment estimates of the spectral displacements at the performance point computed. Finally, the fragility curves for the different DSs were expressed in terms of the standard normal distribution function. Table 1 summarizes the medians and lognormal standard deviations obtained in each direction for each DSs. The plots of the fragilities are shown in Fig. 5. It can be observed that in the Y-direction the medians are significantly lower, hence these values are recommended for implementation of this building typology.



Table 1 – Summary of fragility curve parameters for typology A

	X-Direction		Y-Direction	
	$S_{d,DS}(m)$	$\beta_{DS}$	$S_{d,DS}(m)$	$\beta_{DS}$
Slight (S)	0.010	0.46	0.009	0.45
Moderate (M)	0.027	0.52	0.021	0.53
Extensive (E)	0.056	0.52	0.051	0.55
Complete (C)	0.226	0.85	0.184	0.79

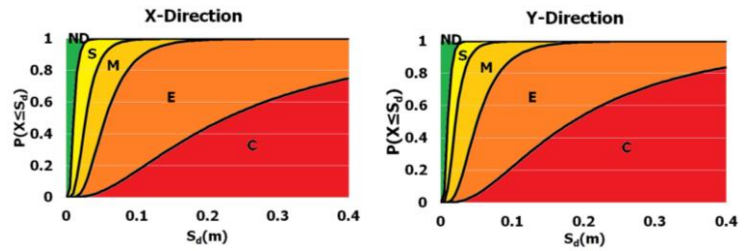


Fig.5- Derived fragility curves, typology A

Fragility curves obtained were compared with those given in HAZUS for a mid-rise RC frame with unreinforced masonry infills (typology C3M), for the pre-code seismic design level (Fig. 6). This comparison should be made with caution, since the fragility curves in HAZUS were derived for US practice and do not consider certain particularities of the present structure, such as distribution of infills, column strength and stiffness irregularities, slab typology, material properties, etc. It can be seen that, overall, the calculated fragilities present lower medians, i.e. higher probability of collapse.

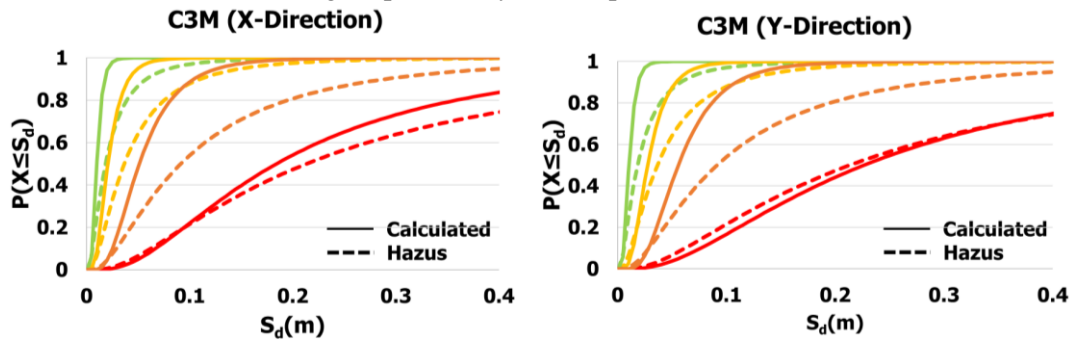


Fig.6- Comparison of calculated and HAZUS fragility curves for typology A

## 4.2. Building typology B

The building is a 4-storey RC frame with infills and flat slabs (Fig. 1), separated by two construction joints (see Fig. 7). 20cm thick shear walls are present around the stair-case, which are constructed of poor unreinforced concrete material known as *Debesh*. *Debesh* concrete is a material unique to Israel. It consists of poor concrete (compressive strength  $f_c \approx 15\text{MPa}$ ) widely used in Israel in the 1940s-1960s to build unreinforced (or very lightly reinforced) walls, among other things. Structurally deficient short columns were identified in the basement. Typical column cross-sections are  $20 \times 25\text{cm}^2$  or  $20 \times 30\text{cm}^2$ , with  $\phi 14$  longitudinal reinforcement and  $\phi 5$  stirrups spaced 20-25cm. Flat slabs consist of 14cm (17cm) thick solid concrete slabs with 5cm (7cm) sand topping. The infill panels are assumed consisting of unconfined concrete masonry blocks of dimensions  $100 \times 100 \times 200$  mm with cement mortar applied in the bed and head joints.

The material properties for steel and concrete were obtained from site investigation. The concrete compressive strength and yield strength of steel are assumed to be randomly distributed, with means and standard deviations of  $\mu_{f_c} = 28\text{MPa}$ ,  $\sigma_{f_c} = 4.2\text{MPa}$  for  $f_c$ , and  $\mu_{f_y} = 226\text{MPa}$ ,  $\sigma_{f_y} = 24\text{MPa}$  for  $f_y$ . 10 different sets of strengths were used for analysis.

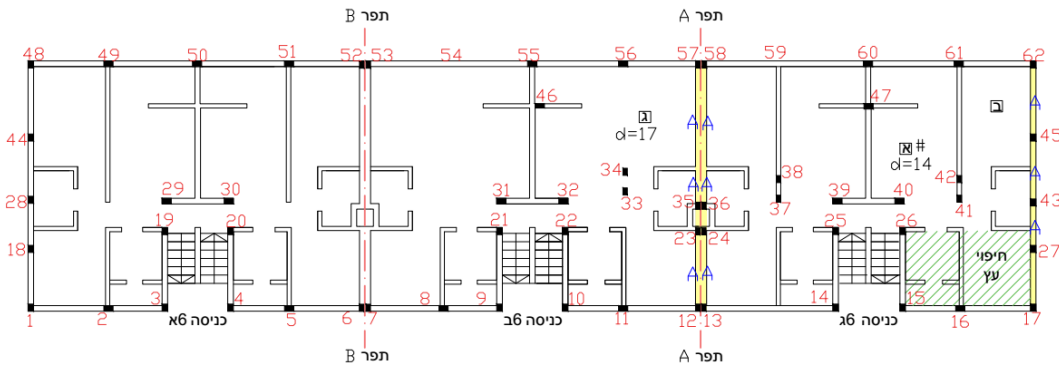


Fig. 7- Building plan configuration, typology B

According to HAZUS, the present building can be classified as mid-rise “Concrete frame with unreinforced masonry walls” (group category C3M). This is a “composite” structural system where the initial lateral resistance is provided by the infill walls. Upon cracking of the infills, further lateral resistance is provided by the concrete frame “braced” by the infill acting as diagonal compression struts. Collapse of the structure results when the infill walls disintegrate (due to compression failure of the masonry “struts”) and the frame loses stability, or when the concrete columns suffer shear failures due to reduced effective height and the high shear forces imposed on them by the masonry compression struts.

Seismic hazard was obtained from probabilistic site-specific assessment, and ground motions were selected as described in section 4.1. The structure was modeled as described in section 4.1, and the same damage criteria as defined in section 4.1 was used.

Results from pushover analysis are shown in Figs. 8, where the top displacement was chosen as the controlling degree of freedom. From **Error! Reference source not found.** it can be noticed that the response in the X direction is more flexible, with a lower capacity but higher ductility. In the y direction the response is stiffer, with a higher capacity but much lower ductility. This difference in the response is mainly due to the orientation of the columns (strong axis in the Y direction), which provides more lever arm to the tension reinforcement, and therefore higher bending moment capacity. Also, the presence of infills affects the response. The collapse mechanisms are shown in Fig. 9. In both directions a soft-story develops above the ground level, with plastic hinging at top and bottom of the columns.

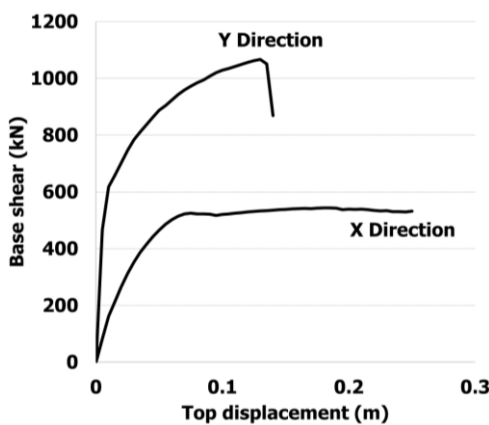


Fig. 8- Pushover curve, typology B

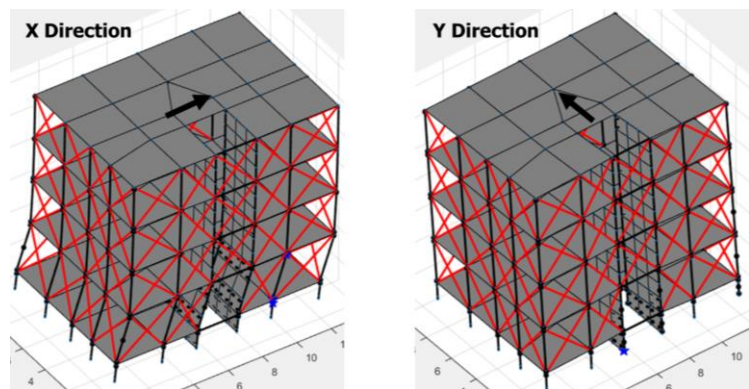


Fig. 9- Soft-story mechanisms at global failure

The maximum IDR damage thresholds associated with each DS were identified on the global pushover curves. Extensive damage was assumed between the point of global yield and peak strength. Slight and moderate damage were assumed between first cracking and global yield, with an equal distribution. . In Fig. 10, the five DSs are highlighted. The maximum IDR thresholds associated with each DS are summarized as follows: 0.12%- “S”, 0.33%- “M”, 0.56%- “E”, 0.65%- “C”- in the X direction, and 0.05%- “S”, 0.14%- “M”, 0.18%- “E”, 0.71%- “C”- in the Y direction.





CSM was used for performance evaluation under different earthquake damage scenarios, where the performance point for each one of the ten structures previously defined, in each direction and for each set of seven scaled ground motions, was computed, and associated to its corresponding DS through the maximum IDR. Table 2 summarizes the medians and lognormal standard deviations obtained in each direction for each DS. The plots of the fragilities are shown in Fig. 10. It can be observed that in the Y-direction the medians are significantly lower, hence these values are recommended for implementation of this building typology.

Table 2 – Summary of fragility curve parameters for typology B

	X-Direction		Y-Direction	
	$S_{d,DS}(m)$	$\beta_{DS}$	$S_{d,DS}(m)$	$\beta_{DS}$
Slight (S)	0.013	0.49	0.005	0.60
Moderate (M)	0.027	0.44	0.011	0.41
Extensive (E)	0.042	0.42	0.026	0.61
Complete (C)	0.223	0.92	0.082	0.48

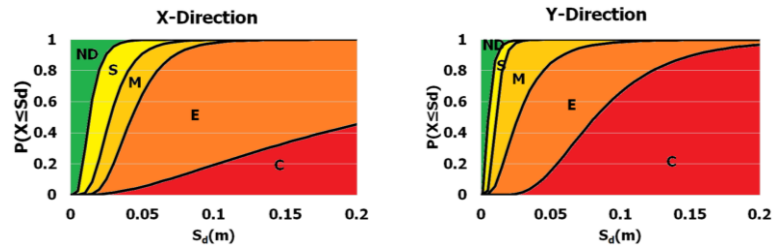


Fig.10- Derived fragility curves, typology B

### 4.3. Building typology C

The typical building is a 4-story structure, 11m height, with a rectangular plan layout of dimensions 15x10m (Figs. 11-12). The structure consists of prefabricated concrete panels connected with non-seismically resistant connectors (intended for lifting and assembly during construction) and slabs without diaphragm action. Some panels present openings for windows and doors, and typically embedded insulation. Based on previous field surveys, these panels present a very brittle behavior under shear forces due to low reinforcement ratios ( $\rho \approx 0.05\%$ ). The structure presents concrete walls at the ground level in both directions, as well as a soft-story created by removal of some panels at the ground level. A frame system is present at this level which supports the above panels. Some walls surrounding the staircase shaft extend up throughout the building, forming a U-shaped core wall. From previous investigations, concrete walls in old buildings were found to be built with *Debesh* material, which consists of very poor quality concrete with compressive strengths of 10-20MPa. Four types of panels were identified in the building: external and internal, without openings and with openings of different configuration. The panel thickness and height are approx. 20cm and 2.80m, respectively. The length is variable, between 2.40-5.10m. Foundation consists of micro-piles with maximum vertical capacity 85 ton.

The concrete compressive strength and yield strength of steel of the cast-in-situ elements were assumed to be randomly distributed, whereas for the precast panels deterministic values area assumed. The mean and standard deviation are  $\mu_{fc}=20\text{MPa}$ ,  $\sigma_{fc}=3\text{MPa}$  for  $f_c$ , and  $\mu_{fy}=250\text{MPa}$ ,  $\sigma_{fy}=15\text{MPa}$  for  $f_y$ . The concrete of the *Debesh* walls was assumed to be of poor quality, whereas for the precast panels a better quality control is expected.

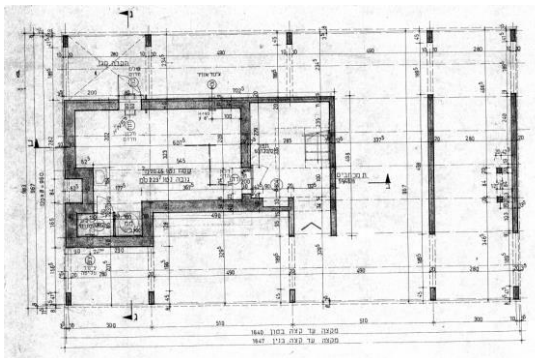


Fig. 13- Building plan configuration, typology C



Fig. 14 Building elevation, typology C



There is no building type in the HAZUS classification corresponding to the present building, which is a mixed system composed of precast panels, RC walls, and RC frames. The most similar classification would be “Precast Concrete Tilt-up Wall” (group category PC1). Damage definitions of HAZUS-PC1 apply only partially to the present building. Elements such as welded connections, plywood or ledger beams are not present in the building. The precast panels analyzed here have a brittle behavior characterized by softening, hence ductile damage mechanisms such as “chord yielding” do not apply. Sliding between panels and RC wall damage was identified prior to failure of connections. Finally, HAZUS-PC1 typology refers to 1-2 story buildings, whereas the present building has 4 stories.

Seismic hazard was obtained from probabilistic site-specific assessment, and ground motions were selected as described in section 4.1. The structure was modeled in the FE software IDEEA, which accounts for geometric and material nonlinearities. Precast panels were modeled with a combination of axial and shear spring elements. Axial springs are rigid links for transferring vertical loads only. Shear springs represent the nonlinear behavior under lateral forces. This is assumed to have a bilinear backbone curve with a maximum strength and a maximum displacement, after which the residual strength is set to zero. In this way, a brittle failure mechanism of the panels can be taken into account. The frame system located at the ground floor was modeled with inelastic beam-column fiber elements. Cross section dimensions were  $0.2 \times 0.45 \text{ m}^2$  for the columns, and  $0.2 \times 0.4 \text{ m}^2$  for the beams. Typical reinforcement ratios as found from previous field investigations were assumed. These were 0.2% for the columns (total longitudinal reinforcement) and 0.1% for the beams (tensile longitudinal reinforcement). Slabs were modeled with elastic elements representing perimeter beams connected to the precast panel elements and concrete (*Debesh*) walls. This case, assuming there is no topping, sets a lower bound of structural behavior under horizontal dynamic loading. Four wall panel types were modeled in detail using nonlinear plane stress (membrane) finite elements. A very low reinforcement ratio of 0.05% was defined for reinforcement in X and Y directions, according to previous studies. The panels were subjected to uniform compression due to gravity loads, which was kept constant during the analysis, and incremental lateral forces. Different levels of compression were investigated depending on the location of the wall. Despite the complexity of different contact mechanisms between precast elements, it was shown that under lateral loading sliding is the critical phenomenon and that connection failure happens after sliding. Here sliding was modeled by friction elements defined between panel elements along the horizontal joint. It was assumed that only the perimeter panels activate friction, i.e. that the interior panels do not contribute to friction and only carry gravity loads. The maximum friction force was estimated from gravity loads acting on the perimeter panels in the X and Y directions.

The damage thresholds corresponding to the DSs defined were identified directly on the pushover curve. The following criteria was adopted: slight damage at first cracking, moderate damage at global yield point, extensive damage at 50% between global yield and sliding, complete damage at sliding.

Results from pushover analysis are shown in Fig. 13. In the X direction, response was dominated by failure of the U-shaped wall and sliding of the panels. In the negative direction a diagonal shear crack was noticed in the U-shaped wall. After wall failure, some redistribution capacity was observed, after which sliding occurred. Although sliding mechanism can be considered as beneficial for energy dissipation in earthquake engineering, by strategically activating it at specific locations, in the present case it is rather “uncontrolled” sliding between panels, which, in reality, will lead to collapse. Hence, once sliding initiates it is considered that the structure reached its collapse state. In the Y direction, in the positive direction, the U-shaped wall presents higher capacity due to the tensile contribution of the flange region. In the negative direction, tension forces in the U-shape wall are carried by the web regions which have comparatively lower tensile capacity. The response was dominated by failure of the U-shaped wall and sliding of the panels. Flexural cracks in the wall were observed in the – Y direction. As before, it was assumed that failure takes place once sliding initiates.

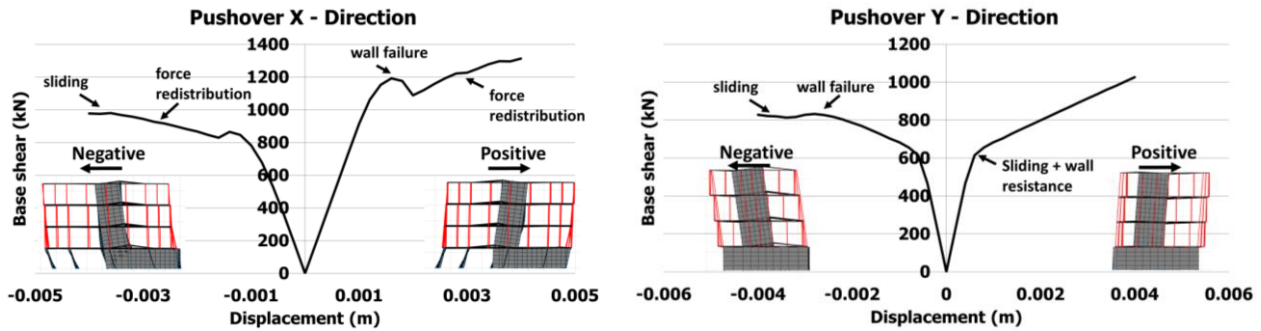


Fig. 13- Pushover curves, typology C

The maximum IDR damage thresholds associated with each DS were identified on the global pushover curves, following the criteria abovementioned. In Fig. 14, five DSs are highlighted. The maximum IDR thresholds associated with each DS are summarized: 0.018%- “S”, 0.045%- “M”, 0.068%- “E”, 0.091%- “C”- in the X direction, and 0.008%- “S”, 0.014%- “M”, 0.039%- “E”, 0.060%- “C”- in the Y direction.

CSM was used for performance evaluation under different earthquake damage scenarios, where the performance point for each one of the ten sample structures previously defined, in each direction and for each set of seven scaled ground motions, was computed, and associated to its corresponding DS through the maximum IDR. Table 3 summarizes the medians and lognormal standard deviations obtained in each direction for each DS. The plots of the fragilities are shown in Fig. 14. It can be observed that in the Y-direction the medians are lower, hence these values are recommended for implementation of this building typology.

Table 1 – Summary of fragility curve parameters for typology C

	X-Direction		Y-Direction	
	$S_{d,DS}(m)$	$\beta_{DS}$	$S_{d,DS}(m)$	$\beta_{DS}$
Slight (S)	0.00065	0.50	0.00041	0.51
Moderate (M)	0.0017	0.55	0.0008	0.42
Extensive (E)	0.0041	0.42	0.00326	0.40
Complete (C)	0.0351	1.57	0.0358	0.88

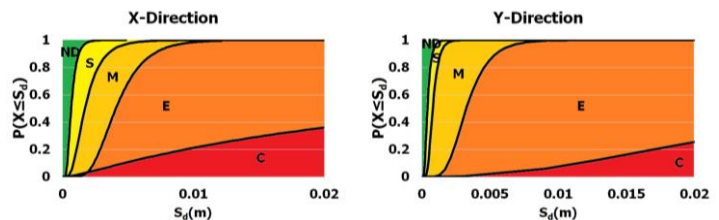


Fig. 14- Derived fragility curves, typology C

A comparison with the fragilities reported in HAZUS for building typology PC1 is shown in **Error! Reference source not found.**15 . It can be seen that the calculated fragilities present much lower spectral displacement medians compared with HAZUS. As mentioned above, typology in HAZUS is significantly different from the present one. Hence a direct comparison is not possible.

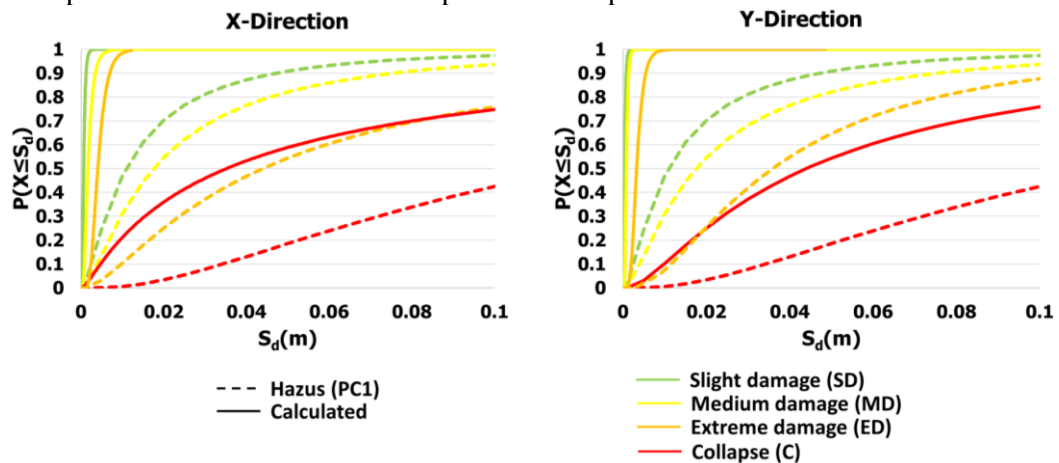


Fig. 15- Comparison of calculated and HAZUS fragility curves for typology C



## 5. Conclusions

Presently, damage and loss estimation on a national level are carried out in the State of Israel using the HAZUS platform, as commonly used in practice worldwide. However, as no fragility curves and parameters relevant to Israeli building stock are currently available, estimations are carried out using HAZUS parameters relevant to US building stock. This results in an unrealistic damage and loss estimation. In order to allow a better estimation of expected damage, which is based on more realistic vulnerability of local building stock, which, in turn, will allow better decision making and preparedness on a national level, this paper focused on the process which allowed derivation of new fragility curves and parameters for three different distinct common Israeli building types. Derivation of fragility curves was based on common practice procedures, which include use of nonlinear pushover analysis and capacity spectrum method to obtain performance points that can be associated with defined damage states of interest. These allow computation of fragility parameters, based on a normal distribution function, while accounting for uncertainties.

Results show that use of US-based fragility parameters leads to un-conservative damage estimation. I.e. it was found that Israeli buildings show more probability of reaching each DS than their US counterpart. This can be the result of poor building material strengths, poor reinforcement detailing, poor connections etc. Results emphasize the need to derivate new fragilities for local building stock, so as to allow more realistic damage and loss estimations as a basis for better preparedness on a national level. To allow further improvement of estimations there is a need to produce additional curves for more typical building types.

## 6. Acknowledgements

The authors would like to acknowledge the financial support of the Israeli National Seismic Preparedness Steering Committee. The authors would also like to thank Dr. Tsafirir Levi and Dr. Rani Calvo from the Geological Survey of Israel for their support regarding the Israeli implementation of HAZUS.

## 7. References

- [1] HAZUS–MH 2.1: Multi-hazard Loss Estimation Methodology- Earthquake Model, Technical Manual, Department of Homeland Security Federal Emergency Management Agency Mitigation Division Washington, D.C.
- [2] Yankelevsky, D., Schwarz, S., Leibovitch, E., and Offir, Y. (2011): Basis for Preparation of Databases Related to Existing Buildings in Israel: Stage I – Residential Buildings. Brussels: Ministry of National Infrastructures and the Technion Research and Development Foundation Ltd.
- [3] Shohet, I., Aharonson-Daniel, L, and Levi, T. (2016): Analytical-Empirical Model for the Assessment of Earthquake Casualties and Injuries in a Major City in Israel – The Case of Tiberias, Geological Survey of Israel, Report No. GSI/21/2016.
- [4] Simoes, D.M.R., Tsionis, G. (2015): Seismic Fragility Curves for the European Building Stock: Review and Evaluation of Analytical Fragility Curves. JRC Technical Report JRC99561.
- [5] ATC, Applied Technology Council (1996): Seismic Evaluation and Retrofit of Concrete Buildings, ATC 40 Report. Redwood City, California, U.S.A.
- [6] IDEEA3D: Nonlinear FEA Software for Earthquake Engineering, 2019. Available at: <https://sites.google.com/site/ideeanalysis>